

BOND GRAPH MODEL OF A POWER REGENERATIVE HYDROSTATIC TRANSMISSION DYNAMOMETER

Biswaranjan Mohanty and Kim A. Stelson

Department of Mechanical Engineering, University of Minnesota, Minneapolis, MN 55455, US
mohan035@umn.edu, kstelson@umn.edu

ABSTRACT

A hydrostatic transmission consists of a hydraulic pump driving a hydraulic motor, a configuration that is commonly used in construction and agricultural equipment. With a superior power-to-weight ratio and continuously variable transmission capability, an HST is an ideal candidate for a wind turbine drivetrain. To validate the performance of an HST as a wind turbine drivetrain, a novel power regenerative HST dynamometer was successfully designed, constructed, and commissioned. The dynamometer is a multi-domain system, consisting of electrical, mechanical, and hydraulic components. Modeling of such multi-energy domains needs a unified and systematic approach. Bond graph modeling is well suited for this complex system. In this paper, a bond graph model of the HST wind turbine and power regenerative dynamometer is developed. The state equations are generated from the bond graph model. The system is ill-conditioned in the limit of incompressibility and no leakage. The input-output coupling is analyzed using the bond graph model.

Keywords: Hydrostatic transmission, Dynamometer, Wind turbine, Bond graph modeling,

1 INTRODUCTION

With the increasing demand for green and renewable energy, wind energy has seen its maximum growth in the last decade. Most utility-scale wind turbines (greater than 1MW) are installed far away from the point of use, increasing transmission cost while incurring about 5% power loss in transmission lines. In contrast, for distributed wind, small (less than 100 kW) and midsize (100 kW to 1 MW) turbines can satisfy local demand and make the electrical grid more reliable and stable. Distributed wind can be used for factories, hospitals, and communities. At present, distributed wind turbines are witnessing slow growth due to high costs of installation, operation, and maintenance (Department of Energy 2018).

Hydraulics are commonly found in high power and high load applications such as construction equipment. The hydraulic transmission consists of a hydraulic pump driving a hydraulic motor. Compared to a heavy, fixed ratio wind turbine gearbox transmission, a hydrostatic transmission (HST) is a cheaper, lighter, and more reliable alternative for wind turbines. A continuously variable HST decouples the turbine generator from the rotor and allows it to rotate at synchronous speed (Mohanty, Dhople and Stelson 2019). The hydraulic components for HSTs in the distributed wind turbines power range are readily available.

To demonstrate and validate the performance of an HST, a power regenerative dynamometer has been built at the University of Minnesota (Mohanty, Wang and Stelson 2019). The dynamometer has two hydrostatic closed loops coupled to each other. Instead of dissipating the output power of the HST, the power is fed back into the system to power a hydrostatic drive. Due to power regeneration, the system consumes less power. The dynamometer has multiple energy domains, consisting of electrical, mechanical, and hydraulic

components. It is integrated with multiple sensors to test hydraulic fluids, components, and controls.

Bond graph modeling is a graphical approach, suited for modeling multi-domain physical systems, where different forms of energy are involved. Bond graphs are domain neutral and were first conceptualized by Paynter (Paynter 1961). The advantage of using bond graphs for power regenerative dynamometer modeling is its unified modeling approach for elements and variables across different energy domains (Karnopp, Margolis and Rosenberg 2012). The bond graph has been applied in complex mechanical and hydraulic systems (Bera, Bhattacharya and Samantaray 2011; Filippa *et al.* 2005; Li, Zhu and Chen 2014). The main objective of this paper is to model the power regenerative dynamometer and analyze the input-output coupling of the system using bond graphs.

2 BOND GRAPH MODELING

The HST wind turbine and the power regenerative dynamometer are multi-domain systems that consist of electrical, mechanical, and hydraulic components. For such electro-hydro-mechanical systems, the bond graph is a powerful method to model the systems in a unified way. The bond graph is a graphical representation of the energy flow in the system. It corresponds to the bi-directional exchange of physical energy and can be incorporated into multiple domains seamlessly. The bond graph notation enables visualization of all aspects of the system effortlessly.

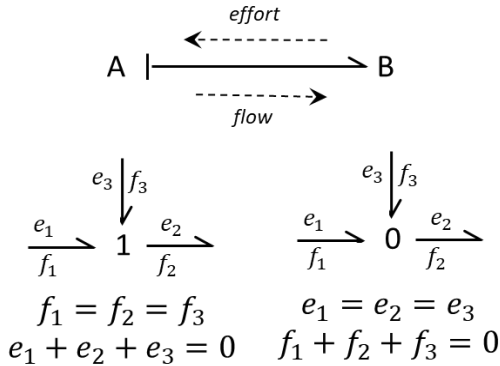


Figure 1: General convention of bond

The bond graph consists of a set of multiports, which are components of a system and its subsystems. Each multiport element is linked to the others by power bonds. Each power bond has an associated effort and flow variable. Each bond has a half arrow sign, showing the direction of the positive power and a casual stroke showing the causality of the effort and flow, as illustrated in Figure 1. The 1-junction is a common flow junction and the 0-junction is a common effort junction. The power variables in electrical, rotary mechanical, and hydraulic systems are listed in Table 1.

Table 1: Bond graph power variable

Power Variable	Electrical	Rotary Mechanical	Hydraulic
Effort, e	Voltage, V	Torque, τ	Pressure, p
Flow, f	Current, i	Angular Speed, ω	Flow, Q

It is instructive to compare energy conversion to rotational mechanical power from electrical or hydraulic power. Energy can be converted between electrical and rotation mechanical domains using an electrical motor/generator. The equations for an idealized motor/generator are:

$$\tau = k_m i, \quad \omega = \frac{1}{k_m} v$$

where k_m is the motor constant. In a motor/generator, torque is proportional to current ($\tau \propto i$) and angular velocity is proportional to voltage ($\omega \propto v$) so that a motor/generator is a gyrator.

Energy can be converted between hydraulic and rotation mechanical domains using a hydraulic pump/motor. The equations for an idealized hydraulic pump/motor are:

$$\tau = \frac{D}{2\pi} p, \quad \omega = \frac{2\pi}{D} Q$$

where D is the pump/motor displacement. In a pump/motor, pressure is proportional to torque ($p \propto \tau$) and flow is proportional to rotational speed ($Q \propto \omega$). In contrast to the electrical

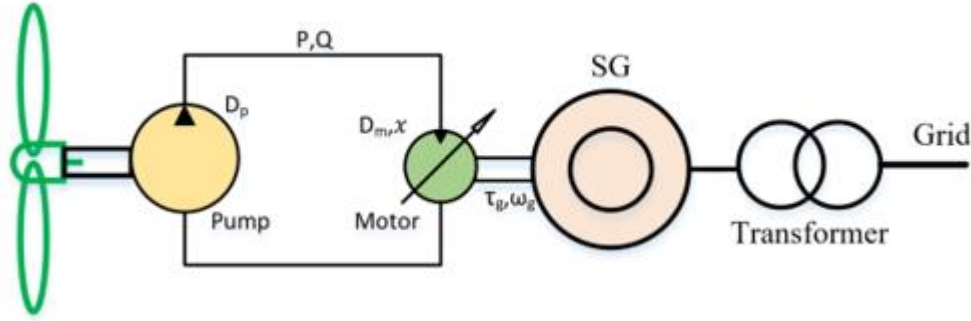


Figure 2: Schematic of a HST wind turbine

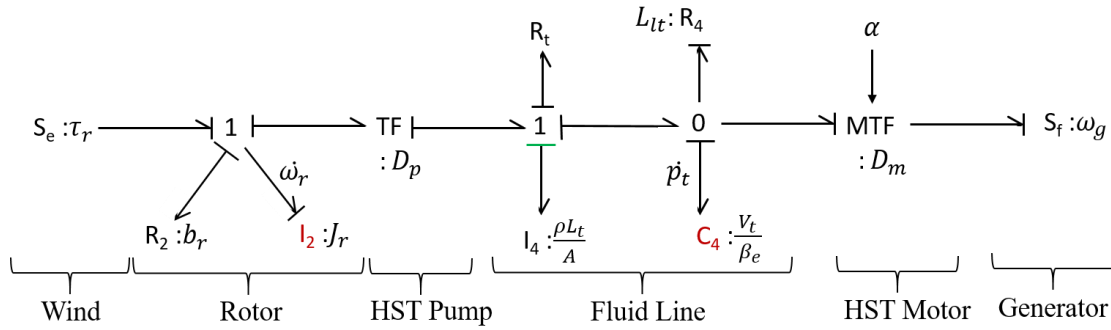


Figure 3: Bond graph of a HST wind turbine

motor/generator, a hydraulic pump/motor is a transformer.

3 HST WIND TURBINE

In an HST wind turbine, a rotor transfers the power from the wind to a synchronous generator through a hydrostatic transmission (HST). The HST consists of a fixed-displacement hydraulic pump and a variable-displacement hydraulic motor. The turbine rotor drives the hydraulic pump to create flow. The hydraulic fluid enters the variable displacement motor to drive the synchronous generator producing electricity. The motor displacement is controlled by an electro-hydraulic proportional valve. The schematic is shown in Figure 2.

A bond graph of the HST wind turbine is shown in Figure 3. The torque applied on the rotor by wind is denoted as an effort source, S_e . The rotor shaft is modeled as a 1-junction, with the inertia of the rotor shaft, I_2 , and a damping coefficient of the rotor shaft, b_r . The fixed-displacement hydraulic pump converts the mechanical rotational power to fluid power and is modeled as a 2-port transformer

(TF). The variable-displacement hydraulic motor converts the fluid power back to rotational power and is modeled as a 2-port modulated transformer (MTF). The transformer moduli are the displacement of the pump, D_p , and the displacement of the motor, αD_m . The displacement of the motor is modulated by a normalized swash plate angle, α , denoted by an active bond. The pump and motor have viscous friction loss and leakage loss. The friction loss is proportional to the rotational speed and is included with the viscous loss, b_r . The leakage loss is proportional to the hydraulic line pressure and is modeled as a resistive element, L_{lt} . Fluid lines are characterized by fluid inductance, I_f , resistance, R_f , and capacitance, C_f , given by

$$I_f = \frac{\rho L}{A}, R_f = \frac{128\eta L}{\pi D^4}, C_f = \frac{\beta_e}{V} \quad (1)$$

$$\frac{1}{\beta_e} = \frac{1}{\beta_f} + \frac{1}{\beta_h} + \frac{a}{1.4p_d}$$

The inductance is a function of the fluid density, ρ , the length, L , and cross-sectional area, A , of the hydraulic line. The resistance, R_f , is a function of

the fluid viscosity, η , length, L , and diameter of the hydraulic line, D . The capacitance, C_f , is a function of the effective bulk modulus, β_e , and the volume of the hydraulic line, V . The effective bulk modulus, β_e , depends on the bulk modulus of the fluid, β_f , bulk modulus of the hose, β_h , and the adiabatic bulk modulus of the entrained air, $1.4p_a$, where a is the percentage of entrapped air in the total volume (Manring 1997).

The speed, ω_g , of the synchronous generator is modeled as the source of flow, S_f . The positive power flow direction and causality of the HST wind turbine are shown in Figure 3. In the HST wind turbine, power flows from the rotor to the generator. The HST wind turbine has three energy storage elements, I_2 , I_4 , and C_4 . But the fluid inertia, I_4 is not an independent energy storage element, so the system is modeled with two state variables, ω_r , and p_t and an input, α .

4 POWER REGENERATIVE HST DYNAMOMETER

The power regenerative dynamometer has two hydrostatic closed loops coupled to each other, the hydrostatic transmission (HST) under investigation and a hydrostatic drive (HSD) to emulate the rotor torque. The schematic of the dynamometer is shown in Figure 4. In the dynamometer schematic, the HSD is shown on the right and the HST is on the left. The rotor dynamics are simulated from the time-varying wind profile and blade aerodynamics. Unlike a conventional transmission dynamometer where output power is fed to a resistive load, the power

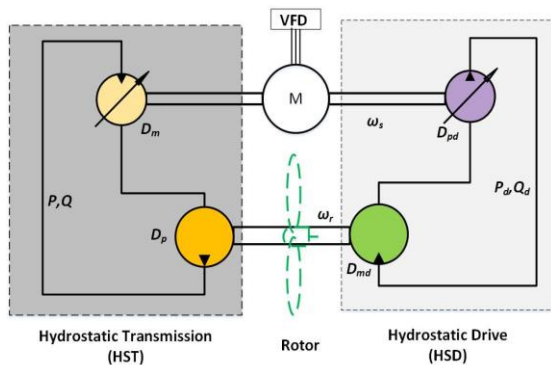


Figure 4: Schematic of power regenerative dynamometer

from the HST drivetrain is fed back to the system to assist the prime mover. An electric motor is installed between the HSD pump and the HST motor to compensate for losses in the circuit. Because of power regeneration, the dynamometer is capable of generating 105 kW of mechanical output with only 55 kW of electrical input. A variable frequency drive (VFD) is used to control the electric motor.

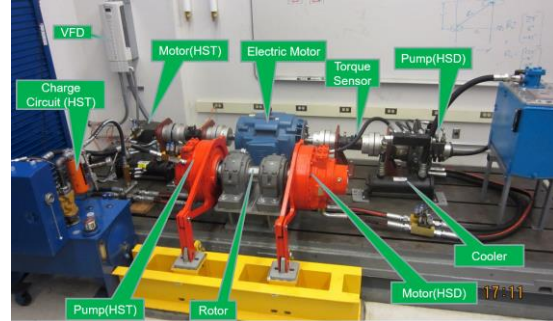


Figure 5: Power regenerative dynamometer developed at University of Minnesota

Similar to the HST, the HSD consists of a variable-displacement pump and a fixed displacement motor. The electric motor along with the HST motor drives the variable displacement pump to create the hydraulic flow. The flow is controlled by an electro-hydraulic proportional valve. The pressurized hydraulic fluid is fed to the fixed displacement motor driving the rotor. The boost pump is integrated with the pump to compensate

Table 2: Key components and parameters of the power regenerative dynamometer

Component	Symbol	Capacity	Description
HSD Pump	D_{pd}	$180 \frac{cc}{rev}$	Variable Axial Piston
HSD Motor	D_{md}	$2512 \frac{cc}{rev}$	Fixed Radial Piston
HST Pump	D_p	$2512 \frac{cc}{rev}$	Fixed Radial Piston
HST Motor	D_m	$135 \frac{cc}{rev}$	Variable Axial Piston
Electric Motor	-	55 kw	Induction Motor

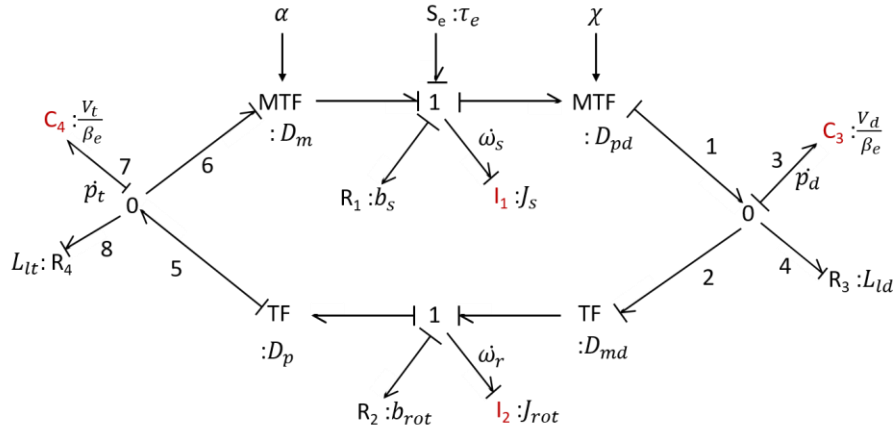


Figure 7: Simplified bond graph model of the power regenerative dynamometer

side of (2)). χD_{pd} and αD_m are transformer moduli. Where, D_{pd} and D_m are the displacement of the HSD pump and HST motor. $\chi \in [0,1]$ is the normalized swash plate angle of the HSD pump and $\alpha \in [0,1]$ is the normalized swash plate angle of the HST motor. The fourth term, $b_s \omega_s$, is a resistive loss, where, b_s is the viscous damping coefficient.

5.2 Low-Speed Shaft (Rotor) Dynamics

From the structure, using effort summation relation, the expression for effort, $\dot{\omega}_r$ is

$$J_{rot} \dot{\omega}_r = D_{md} p_d - D_p p_t - b_{rot} \omega_r \quad (3)$$

$$J_{rot} = J_r + D_{md}^2 \frac{\rho L_d}{A} + D_p^2 \frac{\rho L_t}{A}$$

where J_{rot} is the combined moment of inertia of the rotor, J_r and the HSD and HST fluid inertia. The rotor inertia, J_r is the combined moment of inertia of the rotor shaft, HST pump, and HSD motor. The first term in the right is the torque applied on the rotor shaft by the HSD motor, the second term is the load applied on the rotor shaft by the HST pump. The third term is resistive loss on the rotor shaft. D_p and D_{md} are displacements of the HST pump and the HSD motor, also known as transformer moduli. The combined viscous damping coefficient is b_{rot} .

5.3 HSD Pressure Dynamics

The hydraulic line can be modeled with a fluid capacitance, for the compressibility of the fluid and an inertia element, for the mass of the fluid.

The pressure in the control volume changes due to the difference between the fluids entering and exiting the control volume. The pressure losses in a short fluid line, R_d and R_t are negligible compared to the operating pressure.

Using the flow summation relation and casual sign convention, the equation for the state variable p_d is

$$\frac{V_d}{\beta_e} \dot{p}_d = \chi D_{pd} \omega_s - D_{md} \omega_r - L_{ld} p_d \quad (4)$$

The first and second terms of (4) are the flows from the pump and into the motor, and the third term is the leakage in the HSD system. The volumetric losses in the HSD motor are negligible so that L_{ld} is the leakage loss coefficient of the HSD pump.

5.4 HST Pressure Dynamics

The state equation for p_t is similar to the state equation for p_d . Using the 0-junction constraint and the assigned causality, the equation for the flow variable is

$$\frac{V_t}{\beta_e} \dot{p}_t = D_p \omega_r - \alpha D_m \omega_s - L_{lt} p_t \quad (5)$$

The first and second terms of (5) are the flows from the HST pump and into the HST motor, and the third term is the leakage in the HST system. L_{lt} is the leakage loss coefficient of the HST system. The parameters of the dynamic model are identified from the experiments (Mohanty and Stelson 2018).

6 SYSTEM ANALYSIS

The dynamometer model has four independent energy storage elements with state variables for the high-speed shaft speed, ω_s , the rotor speed, ω_r , the HSD pressure, p_d , and the HST pressure, p_t . The system is controlled by regulating the electric motor torque, τ_e , the HSD pump swash plate angle, χ , and the HST motor swash plate angle, α . The effort source, τ_e , is controlled by the VFD and the control bandwidth is one hundred times faster than the dynamometer system bandwidth. This means that a flow source, ω_s , can replace the combination of effort source, τ_e , inertia, I_1 , and resistive loss, R_1 . The flow on the 1-junction now comes from the flow source rather than the inertia. The causality in the rest of the bond graph is unchanged. The resulting bond graph is shown in Figure 8.

From the state equations, it can be observed that the state, ω_s is multiplied with the inputs, so that the system is non-linear. During HST wind turbine testing, ω_s is the synchronous speed of the generator and is a constant. With a fixed value of ω_s , the system becomes linear with three states and two inputs. The state-space form of the system equations is shown below.

$$\begin{bmatrix} \dot{p}_d \\ \dot{\omega}_r \\ \dot{p}_t \end{bmatrix} = \begin{bmatrix} -\frac{\beta_e L_{ld}}{V_d} & \frac{\beta_e D_{md}}{V_d} & 0 \\ \frac{D_{md}}{J_{rot}} & -\frac{b_{rot}}{J_{rot}} & -\frac{D_p}{J_{rot}} \\ 0 & \frac{\beta_e D_p}{V_t} & -\frac{\beta_e L_{lt}}{V_t} \end{bmatrix} \begin{bmatrix} p_d \\ \omega_r \\ p_t \end{bmatrix} + \begin{bmatrix} \frac{\beta_e D_{pd} \omega_s}{V_d} & 0 \\ 0 & 0 \\ 0 & -\frac{\beta_e D_p \omega_s}{V_t} \end{bmatrix} \begin{bmatrix} \chi \\ \alpha \end{bmatrix} \quad (6)$$

In the dynamometer setup, the HSD motor and HST pumps are identical, meaning that the transformer moduli, D_{md} and D_p are equal, so that the flow on bond 2 ($f_2 = D_{md} \omega_r$) is equal to the flow on bond 5 ($f_5 = D_p \omega_r$).

At a steady-state, \dot{p}_d and \dot{p}_t are zero. Assuming no leakage, $f_8 = f_4 = 0$, the equation for rotor speed,

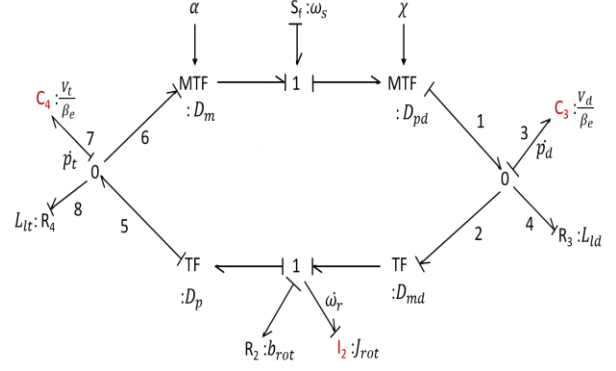


Figure 8: Simplified bond graph

ω_r can be computed from f_1, f_2, f_5 , and f_6 and is given by

$$\omega_r = \frac{D_{pd} \omega_s}{D_{md}} \chi = \frac{D_m \omega_s}{D_p} \alpha \quad (7)$$

From the equation above, it can be concluded that for any change in state variable, ω_r , the HST motor swash plate angle, α and the HSD pump swash plate angle, χ , have to be actuated in a fixed proportion. The inputs are coupled to each other, and the ω_r can not be independently controlled by any single input.

At constant ω_r , the flow at bonds 5 and 2 are identical, $f_5 = f_2 = c$. Assuming no resistive loss in fluid components, $f_8 = f_4 = 0$, the change in the HST and HSD pressure depends on a change in the inputs. From the structure and assigned causality, the equation for a small change in pressure is

$$\Delta p_d = \Delta p_t = \frac{\beta_e D_{pd} \omega_s}{V_d} \Delta \chi = -\frac{\beta_e D_p \omega_s}{V_t} \alpha \quad (8)$$

From the equation above, it can be seen that to increase the HSD and HST pressure we must increase χ and decrease α .

The control objective of the dynamometer is to independently control the HSD and the HST so that the dynamometer can be operated under a wide range of conditions. However, From (7) and (8), we can see that the inputs and outputs of the system are strongly coupled to each other and ill-conditioned so that they are difficult to control independently. Relative gain array analysis can be performed to select an input-output pairing for controller design. A decoupling control can be

designed and implemented to control the HST pressure, p_t , and the rotor speed, ω_r , independently by actuating the HST swash plate angle, α , and HSD swash plate angle, χ . The bond graph analysis reveals that a decoupling controller is required.

7 CONCLUSIONS

The power regenerative hydrostatic dynamometer is a multi-domain system, consisting of electrical, mechanical, and hydraulic components. Modeling of multi-energy domains needs a unified and systematic approach. In this paper, a bond graph model of the dynamometer is developed and dynamical equations are generated. Input-output coupling is analyzed using the bond graph. Inputs and outputs are strongly coupled and it is hard to control the states independently, showing that decoupling control must be used. Bond graph-based modeling provided valuable insight into the power regenerative system dynamics.

ACKNOWLEDGEMENT

This project is funded by the National Science Foundation under grant 1634396. We also thank Eaton, Linde, Danfoss, Bosch Rexroth, Flo-tech, and ExxonMobil for donating the components for the dynamometer. We are thankful to our other graduate students in our lab for helping us in setting up the experiments.

REFERENCES

- Bera, T. K., Bhattacharya, K. and Samantaray, A. K. (2011) ‘Evaluation of antilock braking system with an integrated model of full vehicle system dynamics’, *Simulation Modelling Practice and Theory*. Elsevier, 19(10), pp. 2131–2150.
- Department of Energy (2018) *2018 Distributed Wind Market Report*. Available at: <https://www.energy.gov/eere/wind/downloads/2018-distributed-wind-market-report>.
- Filippa, M. *et al.* (2005) ‘Modeling of a hybrid electric vehicle powertrain test cell using bond graphs’, *IEEE Transactions on Vehicular Technology*. IEEE, 54(3), pp. 837–845.
- Karnopp, D. C., Margolis, D. L. and Rosenberg, R. C. (2012) *System dynamics: modeling, simulation,*

and control of mechatronic systems. John Wiley & Sons.

Li, Y., Zhu, Z. and Chen, G. (2014) ‘Bond graph modeling and validation of an energy regenerative system for emulsion pump tests’, *The Scientific World Journal*. Hindawi, 2014.

Manring, N. D. (1997) ‘The effective fluid bulk-modulus within a hydrostatic transmission’, *Journal of Dynamic Systems, Measurement and Control, Transactions of the ASME*, 119(3). doi: 10.1115/1.2801279.

Mohanty, B., Dhople, S. and Stelson, K. A. (2019) ‘A dynamical model for a hydrostatic wind turbine transmission coupled to the grid with a synchronous generator’, in *Proceedings of the American Control Conference*, pp. 5774–5779. doi: 10.23919/acc.2019.8814746.

Mohanty, B. and Stelson, K. A. (2018) ‘High fidelity dynamic modeling and control of power regenerative hydrostatic wind turbine test platform’, in *BATH/ASME 2018 Symposium on Fluid Power and Motion Control, FPMC 2018*. doi: 10.1115/FPMC2018-8900.

Mohanty, B., Wang, F. and Stelson, K. A. (2019) ‘Design of a Power Regenerative Hydrostatic Wind Turbine Test Platform’, *JFPS International Journal of Fluid Power System*, 11(3), pp. 130–135. doi: 10.5739/jfpsij.11.130.

Paynter, H. M. (1961) *Analysis and design of engineering systems*. MIT press.

AUTHOR BIOGRAPHIES

Biswaranjan Mohanty is a Postdoctoral Researcher in the Neuromodulation Research Center at the University of Minnesota. He holds a Ph.D. in Mechanical Engineering from the University of Minnesota. His research interests lie in system dynamics and control. His email address is mohan035@umn.edu.

Kim A. Stelson is College of Science and Engineering Distinguished Professor in the Mechanical Engineering at the University of Minnesota. He holds an Sc.D. in Mechanical Engineering from M.I.T. His research interests are in fluid power, system modeling and dynamics, and control. His email address is kstelson@umn.edu.